Accepted Manuscript

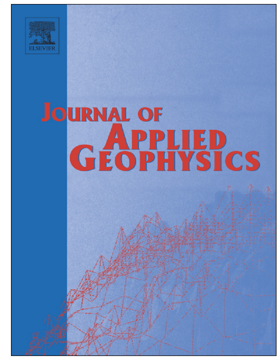

Investigation of the relationship between rock strain and radon concentration in the tidal frequency-range

Gyula Mentes

PII:	S0926-9851(17)30083-6
DOI:	doi:10.1016/j.jappgeo.2018.06.019
Reference:	APPGEO 3547
To appear in:	*Journal of Applied Geophysics*
Received date:	18 January 2017
Revised date:	6 June 2018
Accepted date:	24 June 2018

Please cite this article as: Gyula Mentes , Investigation of the relationship between rock strain and radon concentration in the tidal frequency-range. Appgeo (2018), doi:10.1016/j.jappgeo.2018.06.019

Investigation of the relationship between rock strain and radon concentration in the tidal frequency-range

Gyula Mentes

Geodetic and Geophysical Institute, Research Centre for Astronomy and Earth Sciences, Hungarian Academy of Sciences, Csatkai E. u. 6-8., H-9400 Sopron, Hungary

E-mail address: mentes@ggki.hu Phone: +36-99-508382/Fax: +36-99-508-355.

Abstract

Changes in the radon gas concentration can precede geodynamic processes associated with tectonic, volcanic activities and earthquakes. For this reason the relationship between rock strain and radon concentration is an important scientific issue to be answered. According to the complexity of the radon emanation process influenced by environmental effects, the interpretation of radon concentration variation as a possible precursor of geodynamic processes is not yet resolved unambiguously. The Sopronbánfalva Geodynamic Observatory in Hungary is one of the few places where radon concentration and rock strain variations are simultaneously monitored. The object of this study is to investigate the connection between indoor radon concentration and rock strain in the tidal frequency-range on the basis of seven-year long data series measured in years from 2009 till 2015. The relationship between rock deformation and radon concentration was investigated together with the temperature and barometric pressure effects. It was found that the strain induced radon concentration variations are in the order of 10 – 100 Bq $nstr^{-1}$, while the concentration variations bear more considerable similarity and relation to the temperature and barometric variations. The theoretical tide at the location of the measurement site and tidal components computed from strain, radon concentration, barometric pressure and temperature data were compared with each other. Spectral and tidal analysis of data demonstrated that only the thermally induced solar components S1 and S2 are present in the radon concentration but their amplitudes hardly exceed the spectral noise level. The principal lunar semidiurnal M2 and diurnal O1 tidal waves cause the largest rock strain variations. The lack of the O1 and M2 constituents in the radon concentration confirms the fact that the detected S1 and S2 tidal components appear due to the barometric tide and the daily variations of the temperature and barometric pressure.

Keywords: Earth tide; extensometer; radon concentration; rock strain; underground gallery.

1. Introduction

Radon 222 is an inert, omnipresent radioactive gas which is continuously produced in the rocks and migrates into the air (Steinitz and Piatibratova, 2010; Szabó et al., 2013). Thus the amount of radon exhalation depends on the properties of the rock (elasticity, porosity, permeability, homogeneity, fragmentation, etc.) and on the fractures and hydrologic and geodynamic processes in the rock (Holub and Brady, 1981; Kies et al. 2002, 2005; Millich et al., 1998; Papp et al., 2008). The fact that geodynamic processes also change the properties of rocks, inspires to study geodynamic processes by investigation of radon emanation and concentration. This is why radon concentration variations were observed during volcanic (Toutain and Baubron, 1999; Viñas et al., 2007) and tectonic (Aumento, 2002; Garavaglia et al., 1998, 2000; Mahajan et al., 2010; Omori et al., 2007; Utkin and Yurkov, 2010) activities. Several papers deal with the investigation of the relationship between Earth tides and radon concentration variations measured in underground caves and dwellings (Alekseenko et al., 2010; Barnet et al., 1997a, 1997b; Groves-Kirkby et al., 2004; Kies et al., 1999). Richon et al. (2009) studied the connection between radon concentrations and barometric tides. Since the Earth tide induced local strain in the rock is much smaller than the strain caused by earthquakes, volcanic activity (Viñas et al., 2007) or by large tectonic movements it is difficult to detect the interaction of tidal strain and radon emanations. Furthermore, the amount of radon emanation strongly depends on the temperature and barometric pressure (Barnet et al., 1997a, 1997b; Gregorič et al., 2011; Mentes and Eper-Pápai, 2015; Pinault and Baubron 1996; William and Wilkening 1974). The problem is worsened by the fact that the temperature and the barometric pressure short-term variations coincide with some diurnal and semidiurnal tidal frequencies. In addition, both the temperature and barometric pressure have also an indirect effect, as their changes induce stress in the rock (Mentes, 2000). Until now, the verification of the role of the tidal effect in the radon emanation from rocks and soils has not been reassuringly unambiguous due to the above mentioned problems. Barnet et al. (1997a, 1997b) graphically compared short radon data series with the theoretical tidal components. The short data series and the varying phase shift between the plots questioned the effect of the tidal phenomena. Crockett et al. (2006) calculated the correlation between theoretical tidal signals and radon concentrations but they got very low correlation coefficients (< 0.3). Many authors used FFT (Alekseenko et al., 2010), and additional frequency analysis methods, as spectral-decomposition techniques (Crocket and Gillmore, 2010), Empirical Mode Decomposition, Singular Spectrum Analysis (Crockett et al., 2010), etc. but they came to various results, which can be attributed to different measurement locations and methods. According to our knowledge the relationship between radon concentration and rock strain variations has not yet been investigated using tidal evaluation.

In the Sopronbánfalva Geodynamic Observatory (SGO) simultaneous strain and radon concentration measurements have been carried out by means of a quartz-tube extensometer and an AlphaGUARD™ radon concentration recorder since 2009. It provides a good opportunity to investigate the relationships between strain and radon concentration data. In this paper the relation of radon concentration to rock deformation caused by tidal effects is studied by spectral and Earth tide analysis on the basis of radon concentration, strain, indoor and outdoor temperature and barometric pressure data measured between 2009 and 2015.

2. Observation site and measuring methods

2.1. Observation site

Sopronbánfalva (SGO) is located in the Sopron Mountains near to the Hungarian-Austrian border (see lower right corner in Fig. 1). This territory belongs to the eastern foothills of the Alps represented by crystalline rocks and is characterized by their outcrops in this Alpokalja

(Lower Alps) region. The Sopron Mountains are made of metamorphic rocks of Palaeozoic age such as gneiss and different mica schists which formed from granitic and clastic sedimentary rocks (Kisházi and Ivancsics, 1985, 1987, 1989; Fülöp, 1990; Haas 2001). The reason for the high radon concentration in the SGO is the high uranium and radium concentration in the rocks on this area (Freiler et al., 2015, 2016).

The SGO is an artificial gallery driven horizontally into gneiss in the Nádormagaslat open quarry. The coordinates of the observatory are: latitude 47º40’55’’ N, longitude 16º33’32” E, and the altitude is 280 m a.s.l. The overlay above the gallery is about 60 m. The gallery where the instruments are placed is thermally insulated but not hermetically sealed. There is a slow air transport via the conduit for the electric cables of the instruments. This ventilation does not change the temperature in the gallery but it ensures that the indoor and outdoor barometric pressures are the same. The yearly mean value of the temperature is 10.4 ºC and the yearly and daily temperature variations are less than 0.5 ºC and 0.05 ºC, respectively. The relative humidity of the air is 90% and its variation is negligible. The quarry is not working and there is no human activity in the observatory and in its surroundings. The instruments in the observatory are controlled via Internet.

2.2. Measuring methods

In 1990, a quartz-tube extensometer was installed in the observatory for recording Earth tides and local tectonic movements (Mentes, 1991). Figure 1 shows the ground plan of the observatory and the location of the extensometer in the gallery. The extensometer is about 30 m from the entrance and it is thermally insulated by three doors. The azimuth of the extensometer is 116º and its scale factor is 2.093±0.032 nm mV^{-1}. Construction of the extensometer and its calibration are described by Mentes (2010) in detail.

In autumn 2008, a radon monitor (AlphaGUARD™ PQ2000PRO) was placed near the extensometer (Fig. 1) to measure radon concentrations. The AlphaGUARD™ is able to continuously determine the radon and radon progeny concentrations as well as to register barometric pressure and temperature (http://www.saphymo.com/radiation-measurement/environmental-radiation-monitoring-systems/alphaguard/154.htm, last access: 20.10.2016). AlphaGUARD™ incorporates a pulse-counting ionization chamber (alpha spectroscopy). This instrument is able to measure radon concentrations between 2 Bq m^{-3} and 2 MBq m^{-3}. Its sensitivity is 5 cpm (counts per minute) at 100 Bq m^{-3}. It has a stable long-term calibration factor. The measurements are carried out in diffuse mode. The radon concentration, temperature and barometric pressure data are measured hourly by the radon monitor and are stored in its own memory.

The analogue output signal of the extensometer, the microbarograph, the outdoor temperature and barometric pressure data are sampled and digitized hourly by means of a PREMA 24 bit A/D converter. Radon concentration, strain, outdoor temperature and outdoor barometric pressure data were subjected to data processing, as the indoor temperature was practically constant (10.4 ºC) and the indoor and outdoor barometric pressures did not differ significantly.

3. General overview of the measured data

Figure 2 shows the hourly measured data from 1 January, 2009 till 31 December, 2015. The radon concentration (Rn c.) strongly depends on the outdoor temperature (Temp.) and the measured strain (Strain) also displays a seasonal variation due to temperature variations, while the barometric pressure (Bar. p.) does not have an obvious seasonal character. At first sight, it is apparent that the character of the radon concentration data is different in the summer and winter periods. In the winter months, both the mean value and the variability of the radon concentration is much lower than in the summer months (see also Garavaglia et al., 1998; Gregorič et al., 2011; Mentes and Eper-Pápai, 2015; Przylibski 1999; Virk et al., 2000).

4. Data analysis

Two main methods – spectral and tidal analysis – were applied to detect any connection between radon concentrations and the tides of the solid Earth (Melchior, 1978). The strain, radon concentration, temperature and barometric pressure data were involved into the analyses. For the spectral analysis, Fast Fourier Transformation (FFT) of the data series was used, while the tidal analysis was carried out by the ETERNA 3.40 Earth tide data processing program package (Wenzel, 1996) using the Wahr-Dehant Earth model (Wahr, 1981; Dehant, 1987) and the HW95 tidal potential catalogue (Hartmann and Wenzel, 1995). The program package ETERNA allows the calculation of theoretical tides (e.g. tidal potential and strain for a given location), preprocessing and analysis of Earth tide observation data (gravity, tilt, horizontal, areal and volume strain, and ocean tides). It provides the amplitude factors (measured/theoretical amplitudes) and phase lags between measured and theoretical tidal components in frequency groups depending on the length of the data series. Therefore, the obtained tidal amplitudes by ETERNA may differ from the values obtained from Fourier-transform. The adjusted parameters of the observed tidal strain refer to the Earth model that was used. Beside tidal analysis of strain, radon concentration, temperature, barometric pressure data, ETERNA was used for calculation of theoretical tidal potential and strain data to compare the structure of these signals in the tidal frequency band. Radon gas concentration, temperature and barometric pressure data were analysed as tidal potential data giving adjusted parameters in the original unit. Theoretical strain was calculated as horizontal strain for the azimuth of the extensometer. The data preparation was done by the Tsoft software package for the analysis of time series (Van Camp and Vauterien, 2005). It was used for filtering the data series by a high-pass filter with a cut-off frequency of 0.8 cpd (1 cpd is 1 cycle per day) before Fast Fourier Transformation and by a band-pass filter (low cut-off frequency 0.8 and high cut-off frequency 2.5 cpd) before the tidal analysis. The dependence of the strain and radon concentration on the temperature and barometric pressure was investigated by Multivariable Regression analysis (MVR) using the ORIGIN 9.1 program (http:// www.originlab.com, last access 22.12.2016).

4.1. Results of spectral analysis

Before Fourier analysis, the data were filtered by a high-pass filter (cut-off frequency of 0.8 cpd) to eliminate the disturbing effect of the large, slow variations of data. Figure 3 shows amplitude spectra of the radon concentration (Rn c.) temperature (Temp.), barometric pressure (Bar. p.), measured strain (Ext.) and theoretical strain (Th. strain) data series. Spectra in the diurnal frequency range (0.92–1.05 cpd) are in the left and spectra in the semi-diurnal range (1.92–2.05 cpd) are in the right column. The noise level N in the radon concentration spectrum was calculated as the average of the amplitudes with exception of the largest amplitudes. The theoretical strain spectrum is shown to demonstrate those frequencies where tide generating lunisolar forces act. Fourier amplitudes in the strain, temperature and pressure data are significant, while prominent components of the radon concentration bear much worse signal to noise ratio, especially in the semidiurnal band where these amplitudes can hardly be distinguished from the background spectral noise. Unlike the theoretical and measured strain spectra (second row of the diagrams (Ext.)) which exhibits clear tidal transmission, the radon gas concentration variation produces distinct frequency components only at the S1 (1.000 cpd) and S2 (2.000 cpd) solar harmonics. The amplitude of S1 in the measured and theoretical strain spectra is much smaller (in the noise) than that of the O1 (0.929512006 cpd) principal lunar constituent while it is in inverse relation in the radon concentration spectrum. The largest amplitudes (S1, S2, K1 (1.002925 cpd), K2 (2.005012531 cpd)) in the radon concentration spectrum do not differ essentially from the average noise level (N) and the amplitudes of the principal lunar waves O1, M2 (1.932367 cpd) are below the noise level. The P1 (0.997091815 cpd) principal solar component appears in each data but its amplitude in the measured strain is smaller than its amplitude in the theoretical strain. It can be assumed that the P1 tidal component appears only in the radon concentration data due to the barometric tide.

4.2. Results of the tidal analysis

Tidal analysis was carried out in two different ways. During the first analysis the measured raw data were filtered by the high-pass filter of the ETERNA program (cut-off frequency 0.8 cpd). The temperature (Temp.), barometric pressure (Bar. p.) and radon concentration (Rn c.) data were analysed as tidal potential. The obtained tidal amplitudes are depicted in Fig. 4. Comparing the constituent amplitudes for each data series we can see that the radon concentration variation produces a significant tidal response only in the diurnal K1 (S1) (0.9986-1.0236 cpd) wave group range while in the semi-diurnal band the components are very small. The principal lunar semi-diurnal M2 wave does not appear in the radon concentration. The principal lunar diurnal O1 wave has very small amplitude. The ETERNA program calculates the amplitudes of the individual tidal waves and the standard deviation of their determination. In addition it calculates an average noise level for the diurnal and semidiurnal tidal waves. The amplitudes of O1 and M2 waves are below the noise level in the radon concentration.

Before the second tidal analysis the data were filtered by a band-pass filter to eliminate the disturbing effects of the low and high frequency components of the data series. Since both the rock strain and radon concentration are depending on the temperature and barometric pressure, both were corrected for these quantities in order to compare the corrected and uncorrected radon concentration with the corrected and uncorrected strain values. The correction was done by a multiple linear regression method using the regression coefficients obtained by the MVR. After these corrections the data series were subjected to data analysis by ETERNA. With exception of the strain all data were analysed as tidal potential. The results can be seen in Fig. 5. Due to the correction the amplitude of the S1 in the corrected radon concentration (C. Rn) is smaller than in the uncorrected (Rn), while this is inversely in the corrected (C. Ext.) and uncorrected (Ext) strain components. Since in our observatory the ratios between the amplitudes of the tidal components of the radon concentration and strain are not the same or nearly the same values we can state that there is no significant connection between these two quantities in the diurnal and semidiurnal tidal frequency ranges.

The connection between strain and radon concentration data were also investigated separately for the summer and winter periods. Practically the same results were obtained from the summer months as in the case of the continuous seven-year long data series. In the winter all tidal amplitudes were less than 0.1 kBq m^{-3}, below the noise level.

5. DISCUSSION

In the SGO main lunar diurnal (O1) and semidiurnal (M2) waves, which should be induced by the tidal rock strain, were not detected above the noise level in the radon concentration, while they appear in the theoretical tidal potential and in the strain. In contrast with our results, Lenzen and Neugebauer (1999) detected these two waves in an abandoned gypsum mine, presumably owing to the different measurement site. Steinitz and Piatibratova (2010) also did not reveal the principal lunar waves O1 and M2 near the S1, S2 and S3 components. Crockett et al. (2010) investigated the tidal effect at two measurement sites. At one location they found the weak presence of the M2 wave, while at the other location the wave was not detected. They assume that the S1 and S2 waves are due to the effects of temperature and barometric pressure (e.g. Richon et al., 2009). The S1 and S2 solar tidal components are present in our data similarly to other published results (e.g. Alekseenko et al., 2010; Groves-Kirkby et al., 2006; Kies et al., 1999).

The calculated FFT spectral components and the adjusted tidal amplitudes from the radon concentration data are in good agreement. Both methods show expressed daily variation at only the S1 frequency in the diurnal band and at S2 frequency in the semidiurnal band. The lack of the main solar and lunar components (O1 and M2) is similar to the results of Steinitz and Piatibratova (2010), and together with the presence of the S1 and S2 makes it unambiguous that the tidal rock strain has no direct effect on radon concentration at this location (see Figs. 4 and 5) while the spectral structure of the data series in Fig. 3 and the results of the tidal evaluation support the role of barometric pressure and temperature in the radon concentration variation. The lack of the main lunar components (O1 and M2) in the radon concentration can be explained as follows: while the global effect of tidal forces is considerable (changing the radius of the Earth by 30-50 cm), their local effect is very small. The induced local tidal strain in the rock is in the nanostrain (10^{-9}) range. Therefore its effect on the radon concentration variations is negligible compared to the effect of temperature and barometric pressure variations.

6. CONCLUSIONS

The seven-year simultaneous data record shows a complex relationship between strain, temperature, barometric pressure and radon concentration data. Radon emanation is quite different in the winter and summer. Spectral and tidal analysis of data demonstrated that only the thermally induced solar components S1 and S2 are present in the radon concentration but their amplitudes hardly exceed the spectral noise level. The analysis also proved the lack of the principal lunar semidiurnal M2 and diurnal O1 tidal waves – which have the strongest effect on the deformation of the solid Earth – in radon concentration but they are explicit components in the theoretical tidal and rock strain variations. The lack of the O1 and M2 constituents in the radon concentration confirms the fact that the detected S1 and S2 tidal components appear due to the barometric tide and the daily variations of the temperature and barometric pressure. The investigations do not reveal any significant connection between radon concentration variations and Earth's tide induced rock strain above the noise level at the measurement site.

ACKNOWLEDGEMENTS

This research was funded by the Hungarian National Research Fund (OTKA) under project K 109060.

The author thanks Professor Maurizio Fedi for the careful handling of the manuscript and Professor Carla Braitenberg for her valuable comments which helped to improve the paper. Special thanks are given to Tibor Molnár for his careful maintenance of the instruments and to Ildikó Eper-Pápai for her help in the preparation and pre-processing of data.

REFERENCES

Alekseenko, V.V., Gavriluk, M.Yu., Kuzminov, V.V., Stenkin V.Yu., 2010. Tidal effect in the radon-due neutron flux from the Earth's crust, J. Phys. Conf. Ser. 203 012045.

Aumento, F., 2002. Radon tides on an active volcanic island: Terceira, Azores, Geofis. Int., 41 (4), 499–505.

Barnet, I., Kies, A., Skalsky, L., Procházka, J., 1997a. Radon variations and Earth tides in the unventilated underground spaces, Bull. Chech Geol. Surv., 72 (2), 105–114.

Barnet, I., Procházka, J., Skalský, L. (1997b). Do the Earth tides have an influence on short-term variations in radon concentration? Radiat. Prot. Dosim., 69 (1), 51–60.

Crockett, R.G.M., Gillmore, G.K., 2010. Spectral-decomposition techniques for the identification of radon anomalies temporally associated with earthquakes occurring in the UK in 2002 and 2008, Nat. Haz. Earth Syst. Sci., 10, 1079–1084.

Crockett, R.G.M., Gillmore, G.K., Phillips, P.S., Denman, A.R., Groves-Kirkby, C.J., 2006. Tidal synchronicity of built-environment radon levels in the UK, Geophys. Res. Lett., 33, L05308.

Crockett, R.G.M., Perrier, F., Richon, P., 2010. Spectral-decomposition techniques for the identification of periodic and anomalous phenomena in radon time-series, Nat. Haz. Earth Syst. Sci., 10, 559–564.

Dehant, V., 1987. Tidal parameters for an unelastic Earth. Phys. Earth Planet. Inter., 49, 97–116.

Freiler, Á., Horváth, Á., Török, K., 2015. ^{226}Ra activity distribution of rocks in the Sopron Mts. (West-Hungary). J Radioanal Nucl Chem, 306, 243–247. DOI 10.1007/s10967-014-3914-3.

Freiler, Á., Horváth, Á., Török, K., Földes, T., 2016. Origin of radon concentration of Csalóka Spring in the Sopron Mountains (West Hungary). Journal of Environmental Radioactivity, 151, 174–184.

Fülöp, J., 1990. Magyarország geológiája. Paleozoikum I., (Geology of Hungary. Palaeozoic I.), pp. 326, Hungarian Geological Institute, Budapest (in Hungarian).

Garavaglia, M., Braitenberg, C., Zadro, M., 1998. Radon monitoring in a cave of North-Eastern Italy, Phys. Chem. Earth., 23 (9-10), 949–952.

Garavaglia, M., Dal Moro, G., Zadro, M., 2000. Radon and tilt measurements in a seismic area: Temperature effects, Phys. Chem. Earth. (A), 25 (3), 233–237.

Gregorič, A., Zidanšek, A., Vaupotič, J.,2011. Dependence of radon levels in Postojna Cave on outside air temperature, Nat. Haz. Earth Syst. Sci., 11, 1523–1528.

Groves-Kirkby, C.J., Denman, A.R., Crockett, R.G.M., Phillips, P.S., 2004. Periodicity in domestic radon time series – evidence for Earth tides, 11th International Congress of the International Radiation Protection Association, Madrid, Spain, 23-28 May, 2004., irpa11.irpa.net/pdfs/6a26.pdf, 1–10.

Groves-Kirkby, C.J., Denman, A.R., Crockett, R.G.M., Phillips, P.S., Gillmore, G.K., 2006, Identification of tidal and climatic influences within domestic radon time-series from Northamptoshire, UK, Sci. Total Environ., 367 (1), 191–202, doi:10.1016/j.scitotenv.2005.11.019.

Haas, J. (ed.), 2001. Geology of Hungary. Eötvös University Press, Budapest.

Hartmann, T., Wenzel, H.G., 1995. The HW95 tidal potential catalogue, Geophys. Res. Lett., 22 (24), 3553–3556.

Holub, R.F., Brady, B.T., 1981. The effect of Stress on Radon Emanation from Rock, J. geophys. Res., 86, 1776–1784.

Kies, A., Majerus, J., D'Oreye, L., 1999. Underground radon gas concentrations related to Earth tides, Il Nuovo Cimento C, 22 (3-4), 287–294.

Kies, A., Massen, F., Tosheva, Z., 2002. Influence of variable stress on underground radon concentrations, Geofis. Int., 41 (3), 325–329.

Kies, A., Massen, F., Tosheva, Z., 2005. Influence of variable stress on underground radon concentrations, Radioactivity of the Environment, 7, 334–329.

Kisházi, P., Ivancsics, J., 1985. Genetic petrology of the Sopron crystalline schist sequence, Acta Geol. Hun., 28, 191–213.

Kisházi, P., Ivancsics, J., 1987. A Soproni Csillámpala Formáció genetikai kőzettana. Földtani közlöny 117, 203–221.

Kisházi, P., Ivancsics, J., 1989. A Soproni Gneisz Formáció genetikai kőzettana. Földtani közlöny 119, 153–166.

Lenzen, M., Neugebauer, H. J., 1999. Measurements of radon concentration and the role of Earth tides in a gypsum mine in Walferdange, Luxemburg, Health Physics, 77 (2), 154–162.

Mahajan, S., Walia, V., Bajwa, B.S., Kumar, A., Singh, S., Seth, N., Dhar, S., Gill, G.S., Yang, T.F., 2010. Soil-gas radon/helium surveys in some neotectonic areas of NW Himalayan foothills, India, Nat. Hazards Earth Syst. Sci., 10, 1221–1227.

Melchior, P., 1978. The Tides of the Planet Earth, pp.609, Pergamon Press, Oxford.

Mentes, Gy., 1991. Installation of a quartz-tube extensometer at the Sopron observatory, Bull. d'Inf. Marées Terr., 110, 7936–7939.

Mentes, Gy., 2000. Influence of temperature and barometric pressure variations on extensometric deformation measurements at the Sopron Station. Acta Geod: Geoph. Hung., 35 (3), 277–282.

Mentes, Gy., 2010. Quartz tube extensometer for observation of Earth tides and local tectonic deformations at the Sopronbánfalva Geodynamic Observatory, Hungary, Rev. Sci. Instrum., 81, 074501.

Mentes, Gy., Eper-Pápai, I., 2015. Investigation of temperature and barometric pressure variation effects on radon concentration in the Sopronbánfalva Geodynamic Observatory, Hungary, Journal of Environmental Radioactivity, 149, 64–72.

Millich, E., Neugebauer, H.J., Huenges, E., Nover, G., 1998. Pressure dependence of permeability and earth tide induced fluid flow, Geophys. Res. Lett., 25 (6), 809–812.

Omori, Y., Yasuoka, Y., Nagahama, H., Kawada, Y., Ishikawa, T., Tokonami, S., Shinogi, M., 2007. Anomalous radon emanation linked to preseismic electromagnetic phenomena, Nat. Hazards Earth Syst. Sci., 7, 629–635.

Papp, B., Deák, F., Horváth, Á., Kiss, Á., Rajnai, G., Szabó, Cs., 2008. A new method for the determination of geophysical parameters by radon concentration measurements in bore-hole, J. Environ. Radioactiv., 99, 1731–1735.

Pinault, J.-L., Baubron, J.-C., 1996. Signal processing of soil gas radon, atmospheric pressure, moisture, and soil temperature data: A new approach for radon concentration modelling, J. geophys. Res., 101, 3157–3171.

Przylibski, T.A., 1999. Radon concentration changes in the air of two caves in Poland, J. Environ. Radioactiv., 45, 81–94.

Richon, P., Perrier, F., Pili, E., Sabroux, J.-C., 2009. Detectability and significance of 12 hr barometric tide in radon-222 signal, dripwater flow rate, air temperature and carbon dioxid concentration in an underground tunnel, Geophys. J. Int., 176, 683–694.

Steinitz, G., Piatibratova, O., 2010. Radon signals at the Roded site, southern Israel, Solid Earth Discuss., 2, 161–193. doi:10.5194/sed-2-161-2010.

Szabó, K.Zs., Jordan, Gy., Horváth, Á., Szabó Cs., 2013. Dynamics of soil gas radon concentration in a highly permeable soil based on a long-term high temporal resolution observation series, J. Environ. Radioactiv. 124, 74–83.

Toutain, J.-P., Baubron, J.-C., 1999. Gas geochemistry and seismotectonics: a review, Tectonophysics, 304, 1–27.

Utkin, V.I., Yurkov, A.K., 2010. Radon as a tracer of tectonic movements. Russ. Geol. Geophys., 51 (2), 220–227. doi:10.1016/j.rgg.2009.12.022.

Van Camp, M., Vauterin, P., 2005. Tsoft: graphical and interactive software for the analysis of time series and Earth tides, Computers & Geosciences, 31(5) 631–640, doi:10.1016/j.cageo.2004.11.015

Viñas, R., Eff-Darwich, A., Soler, V., Martín-Luis, M.C., Quesada, M.L., de la Nuez, J., 2007. Processing of radon time series in underground environments: Implications for volcanic surveillance in the island of Tenerife, Canary Islands, Spain, Rad. Meas., 42, 101–115.

Virk, H.S., Walia, V., Sharma, A.K., Kumar, N., Kumar, R., 2000. Correlation of radon anomalies with microseismic events in Kangara and Chamba valleys of N-W Himalaya, Geofis. Int., 39(3), 221–227.

Wahr, J.M., 1981. Body tides on an elliptical, rotating, elastic and oceanless Earth, Geophys. J. R. Astr. Soc., 64, 677–703.

Wenzel, H.G., 1996. The nanogal software: Earth tide data processing package ETERNA 3.30, Bull. d'Inf. Marées Terr., 124, 9425–9439.

William, E.C., Wilkening, M.H., 1974. Atmospheric pressure effects on ^{222}Rn transport across the Earth-air interface, J. geophys. Res., 79 (33), 5025–5029.

Figure captions

Fig. 1. Ground plan and the location of the Sopronbánfalva Geodynamic Observatory (SGO) in Hungary (lower right corner)

Fig. 2. Strain measured by the extensometer (Strain), outdoor temperature (Temp.), barometric pressure (Bar. p.) and radon concentration (Rn c.) measured between 1 January 2009 and 31 December 2015

Fig. 3. Fourier amplitude spectrum of radon concentration (Rn c.), barometric pressure (Bar. p.), temperature (Temp.), extensometric data (Ext.) and calculated theoretical strain (Th. strain) in the diurnal (left hand column) and in the semi-diurnal (right hand column) frequency band. N denotes the noise level.

Fig. 4. Amplitudes of tidal components obtained by tidal analysis of the strain (Ext.), temperature (Temp.), barometric pressure (Bar. p.) and radon concentration data (Rn c.)

Fig. 5. Amplitudes of tidal components obtained by tidal analysis of the strain (Ext.), corrected strain for the temperature and barometric pressure (C. Ext), temperature (Temp.), barometric pressure (Bar. p.), radon concentration (Rn) and radon concentration corrected for the temperature and barometric pressure (C. Rn) data

Highlights

- Relationships between rock strain an radon concentration are investigated.
- Temperature and air pressure have a large effect on the radon concentration.
- O1 and M2 tidal constituents in the rock strain are not present in the Rn concentration.
- In the Rn concentration the S1 and S2 solar tidal components are only present.

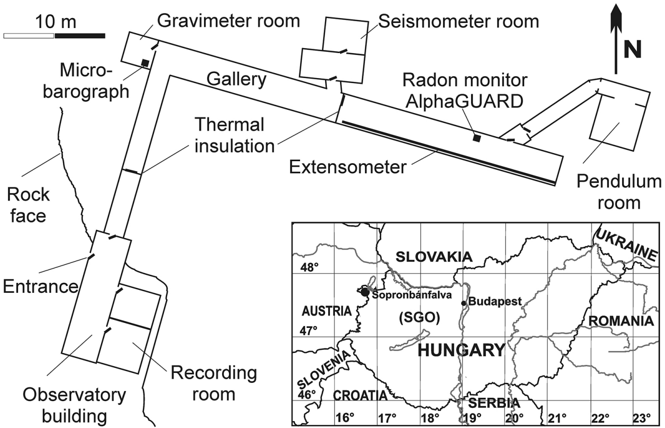

10 m
Gravimeter room
Seismometer room
N
Micro-
barograph
Gallery
Radon monitor
AlphaGUARD
Thermal
insulation
Extensometer
Pendulum
room
Rock
face
Entrance
Recording
room
Observatory
building
SLOVAKIA
UKRAINE
48°
Sopronbánfalva
Budapest
AUSTRIA
(SGO)
ROMANIA
47°
HUNGARY
SLOVENIA
46°
CROATIA
SERBIA
16°
17°
18°
19°
20°
21°
22°
23°

Figure 1

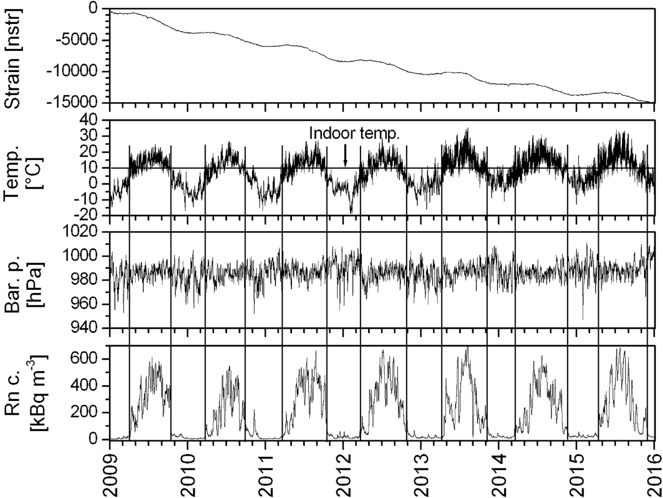
Strain [nstr]
0
-5000
-10000
-15000
Temp. [°C]
40
30
20
10
0
-10
-20
Indoor temp.
Bar. p. [hPa]
1020
1000
980
960
940
Rn c. [kBq m^{-3}]
600
400
200
0
2009
2010
2011
2012
2013
2014
2015
2016

Figure 2

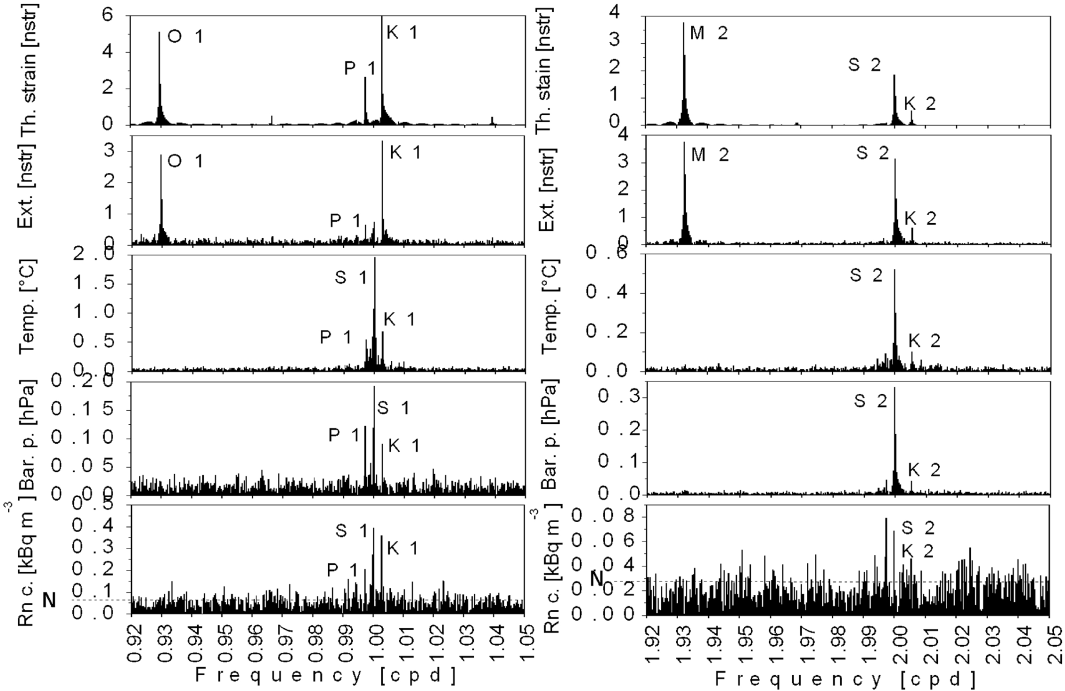
Th. strain [nstr]
O 1
P 1
K 1
Ext. [nstr]
Temp. [°C]
S 1
Bar. p. [hPa]
Rn c. [kBq m^{-3}]
N
M 2
S 2
K 2
Th. stain [nstr]
Frequency [cpd]

Figure 3

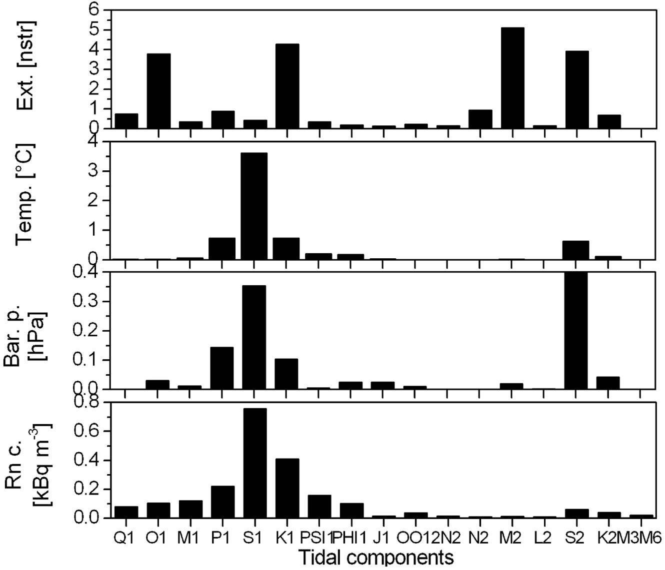

Ext. [nstr]
Temp. [°C]
Bar. p. [hPa]
Rn c. [kBq m-3]
Q1 O1 M1 P1 S1 K1 PSI1 PHI1 J1 OO1 2N2 N2 M2 L2 S2 K2 M3 M6
Tidal components

Figure 4

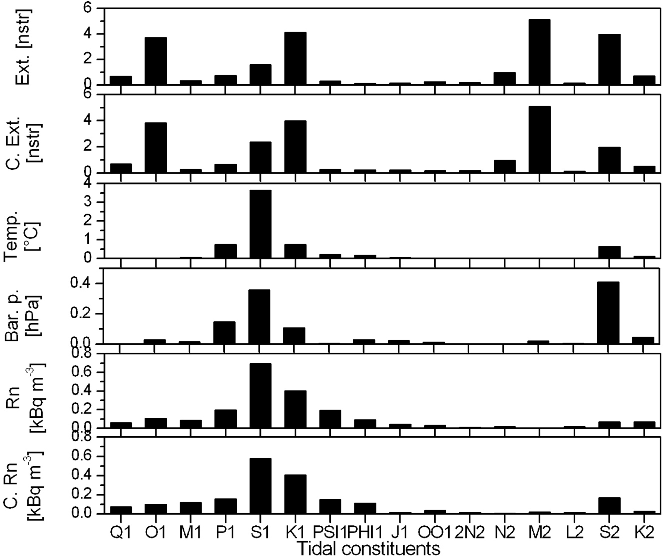
Ext. [nstr]
C. Ext. [nstr]
Temp. [°C]
Bar. p. [hPa]
Rn [kBq m-3]
C. Rn [kBq m-3]
Q1 O1 M1 P1 S1 K1 PSI1 PHI1 J1 OO1 2N2 N2 M2 L2 S2 K2
Tidal constituents

Figure 5